KSCE Journal of Civil Engineering
Vol. 11, No. 3 / May 2007
pp. 133~139

Pore Size Distribution of Pusan Clay Measured by Mercury Intrusion Porosimetry

By Enebish Ninjgarav*, Sung-Gyo Chung**, Woo-Young Jang***, and Choon-Kil Ryu****

Abstract

Little attention was paid to the micro-structural investigation, although a number of geotechnical investigations have been performed on Pusan clay since early 1990s. Particularly, pore size distribution (PSD) which affects permeability, consolidation, and strength and so on has seldom been investigated on the clay. In order to examine the PSD during consolidation, mercury intrusion porosimetry (MIP) investigation was carried out on intact clay and also the one-dimensional consolidated clays with various stress levels, as well as scanning electron microscope (SEM). As the result, the PSD of intact clay was observed in depth and also the change with the applied consolidation stress levels. It was recognized that the PSD are remarkably different for the upper and lower clays, but the compression occurred during consolidation stress is dominantly resulted from a decrease in the inter-aggregate (large) pore spaces (larger than 2 μm in diameter). Moreover, characteristics of the PSD were effectively represented by the mean pore size (D_{p50}).

Keywords: *Pusan clay, MIP, microstructure, pore size distribution, consolidation*

1. Introduction

The Nakdong River plain has elevations varying from 2 to 3m above the mean sea level (MSL). The soil deposit overlying the bedrock consists of loose sand, Holocene silty clay and sandy soil layers. The clay is called 'Pusan clay' (or 'Busan clay'), whose thickness varies from 20 to 40m but can reach 70 to 80m in some locations, especially at the mouth of the river. The top sand layer often disappeared at the locations far away from the main river. The clay consists of upper soft clay that is usually situated above the depth of 30 m and lower stiff or hard clay below the depth. Depending on the location, a thin sand layer is sometimes sandwiched between the both clays.

Since early 1990s, a large number of geotechnical investigations have been performed in the Nakdong River plain. Nevertheless, local practicing geotechnical engineers have not understood clearly the geotechnical characteristics of Pusan clay, so that some researchers have been focused to study on the engineering geology, sampling techniques, in-situ testing and so on during the last decade (Chung et al., 2002; 2003; 2004; 2005a; 2005b). However they have paid little attention to investigating the micro-structural characteristics of the clay, particularly during consolidation.

The purposes of this study were to observe the micro-structure of intact Pusan clay and its change during one-dimensional consolidation, especially for the pore size distribution. The investigation was carried out using the Mercury Intrusion Porosimetry (MIP) technique. The samples were prepared from intact soil and one-dimensionally consolidated soils at various stress levels. An appropriate sample preparation was conducted based on the preliminary investigation. Through the investigation, the pore size distribution of intact Pusan clay and its change of the consolidated clay were observed and compared with clays from other parts of the world. Furthermore, the results were discussed and correlated with void ratio.

2. Basic Geotechnical Properties

For the study, the Hwajeon (HJ) site where is located near-shore was chosen, as shown in Fig. 1. The site was started to reclaim for industrial complex, from the middle of 2006. Fig. 2 presents the basic geotechnical soil properties at the borehole BH-9 of HJ site, including the index properties and CPTU profiles that vary depending on their depositional environment. The values of specific gravity, G_s, was in the range of 2.62~2.70 for the entire depths. The unit weight decreases from 17~18kN/m^3 at the top to 15.5kN/m^3 at the bottom of the upper clay, whereas the value is almost constant with the range of 17~18kN/m^3 in the lower clay. The liquidity index ranges between 0.7~1.5 in the upper clay, while it decreases from 0.4 to 1.2 with depth in the lower clay. The Atterberg limits were performed using fall-cone test and the samples used were air-dried. Detailed information about these can be seen in Chung et al (2006a and 2006b).

3. MIP (Mercury Intrusion Prosimetry) Test

3.1 Principles of MIP Test

Pore size can be determined using the technique of mercury

*Associate Professor, Mongolian University of Science and Technology, Civil Engineering School, Ulaanbaatar, Mongolia
**Member, Professor, School of Civil Engineering, Dong-A University, Busan, Korea
***Member, Manager, GS Engineering & Construction, Seoul, Korea (Corresponding Author, E-mail: jwy1357@hanmail.net)
****Researcher, Institute of Construction Technology and Planning, Dong-A University, Busan, Korea

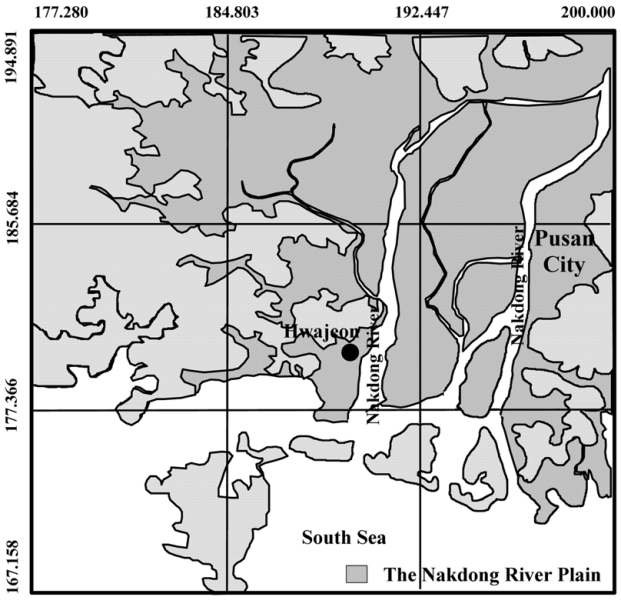

Fig. 1. Location of the Study Area

penetration, which is based on the behavior of "non wetting" liquids in capillaries. Diameter of voids is calculated according to the capillary force theory when mercury is intruded into voids by applying pressure. For this, the following assumptions are needed to consider: (i) The surface tension of mercury and contact angle with solid material are constant during the analysis. (ii) The intrusion pressure must be equilibrium. (iii) Pores are considered as being of cylindrical shape. And (iv) Solids are not subject to deformation under the effect of pressure.

By measuring the quantity of mercury penetrated into the sample pores and the equilibrium pressure at which intrusion occurs, the pore volume distribution as a function of their radius were obtained. A liquid coming in contact with a solid porous material and behaving as a non-wetting agent (if the contact angle of the liquid with a solid material exceeds 90º) cannot be spontaneously absorbed by the pores of the solid itself because of surface tension. However this resistance to penetration can be overcome by the applying external pressure. Required pressure depends on the pore size.

The relation between pore size and applied pressure, assuming the pore is cylindrical, is expressed as (Washburn, 1921):

$$P = \frac{-2T\cos\theta}{r} \tag{1}$$

where P: absolute applied pressure, T: surface tension, θ: contact angle, and r: pore radius.

3.2 Mercury Porosimeter

Mercury Porosimeter used for this study, which was developed by the Thermo Finnigan, Italy was as: Pascal 140+440; pressure range = 0.1~400 MPa, pore radius range = 7500~1.8 nm; and particle diameter range = 40~0.01 m. In the Porosimeter Pascal 140, the mercury volume penetrating the sample pores is measured by means of a capacitive system, while the penetration pressure is measured by an appropriate transducer. The Porosimeter consists of four parts: (i) dilatometer that contains the sample to be analyzed, (ii) pressurization system that includes the peristaltic pump for air and the peristaltic pump for vacuum, (iii) depressurization system that includes the peristaltic pump for air and the peristaltic pump for vacuum, and (iv) measuring system of capacity and pressure that measures mercury intrusion into the sample and the intrusion pressure.

3.3 MIP Testing Program and Sample Preparation

3.3.1 Testing Program

Undisturbed (UD) samples were retrieved from five depths of 14, 18, 24, 29 and 38 m, at a borehole BH-9 of HJ site. Five specimens at each depth were prepared for oedometer testing and also the MIP and scanning electron microscope (SEM) techniques. The standard oedometer test (the load increment of 1.0 and the duration of 24 hrs) was performed up to the appointed stress levels (as described in 3.3.2) and then the samples were removed after releasing the consolidation stresses. Test specimens were prepared by cutting the consolidated and

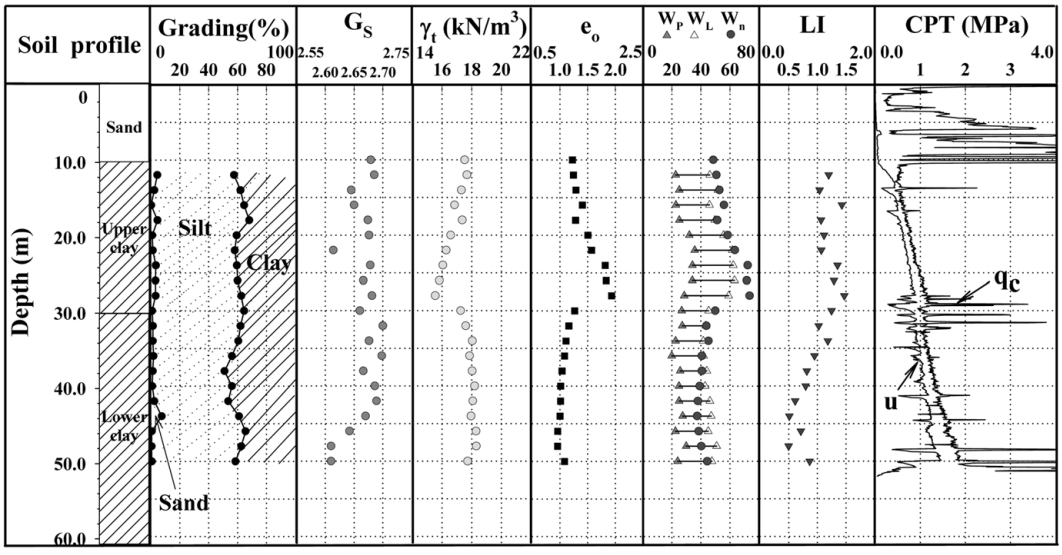

Fig. 2. Typical Geotechnical Properties at the HJ Site (BH-9)

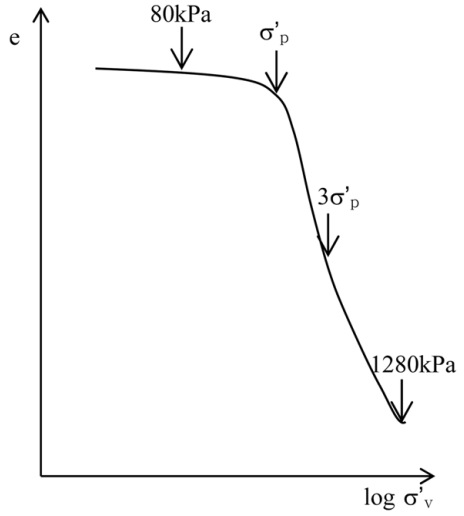

Fig. 3. Scheme of Stress Level for PSD Measured

undisturbed samples, and then tested by the MIP and SEM. Finally, the testing results were analyzed on Pusan clay and also compared with other clays.

3.3.2 Sampling of Test Specimens

Test specimens were obtained from intact and one-dimensional consolidated samples. The consolidation stress levels for the sampling were as below and also as shown in Fig. 3:

① The undisturbed sample ($\sigma_v = 0$)
② A stress level that is less than the consolidation yield pressure (80 kPa)
③ A stress that is about the consolidation yield pressure σ_p'
④ A stress that is about three times as large as σ_p'
⑤ The vertical stress of 1280 kPa.

3.3.3 Treatment of Test Specimens

Mercury Intrusion Porosimetry (MIP) and Scanning Electron Microscope (SEM) techniques require the use of dehydrated sample. There are two kinds of sample preparation: freeze-cut-drying and freeze-drying fracture. The former is to freeze samples, cut using a sharp knife and then dry in the freeze vacuum dryer, whereas the latter is to cut after freezing and drying them. At the preliminary test, the method of freeze-drying-fracture led to a better result than freeze-cut-drying, so that the former method was adopted.

Samples retrieved from the ground were trimmed using a wire saw, for oedometer and MIP tests. Test specimens were prepared from the undisturbed and consolidated samples. No attempt was made to prevent the expansion of specimens during the preparation. That is, the consolidated samples were released from the consolidation stress and then removed from oedometer cell. The samples were submerged in the liquid nitrogen to freeze and then cut for the test specimen. They were in turn put into the freeze vacuum dryer, in which pore water sublimated without volume change. Then, the test specimens were kept in the vacuum desiccator and then de-aired by vacuum pump until the MIP test is performed.

4. Testing Results and Discussion

4.1 Pore Size Distribution (PSD) for Intact Clay

Mercury intrusion porosimetry measures pore sizes over a range of three or more orders of magnitude. The detailed procedure for the measurement was described by Ninjgarav (2006). Fig. 4 presents the intruded porous volume (V) vs. the pore diameter at different depths of the HJ site. It is very interesting to note that for all the curves, the starting magnitude of larger entrance pore diameter is approximately 1 mm, as shown on St. Marcel clay (Delage and Lefebvre, 1984). It is shown that the upper clay has larger pore sizes than the lower clay layer, because of the increase in effective overburden pressure σ_{vo}' and different depositional environments.

Fig. 5 shows the cumulative volume versus pore diameter curves for the intact upper and lower clays at the HJ site. It revealed that there is a difference in the cumulative pore volumes between the upper and lower clays. This is a similar trend as shown in Fig. 4.

The pore size distribution (PSD) of intact clay at different depths is presented in Fig. 6. The ordinate in the plot is dV/(log

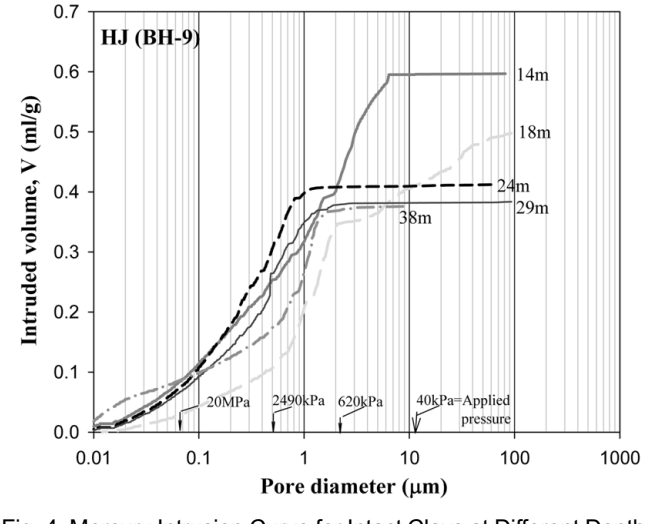

Fig. 4. Mercury Intrusion Curve for Intact Clays at Different Depths

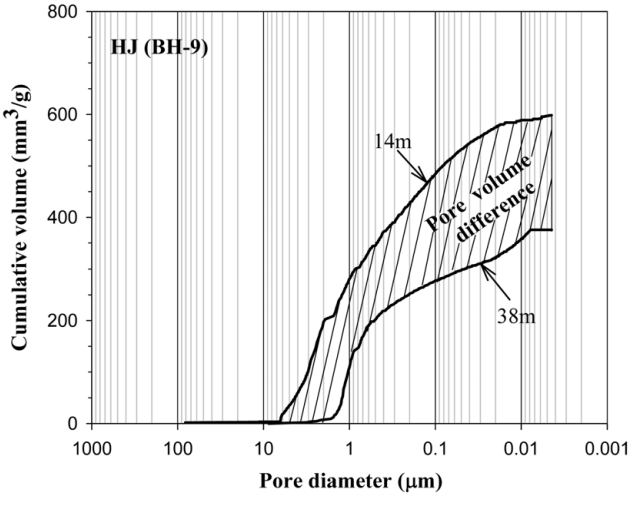

Fig. 5. Cumulative Intrusion Versus Pore Diameter for Intact Upper and Lower Clays

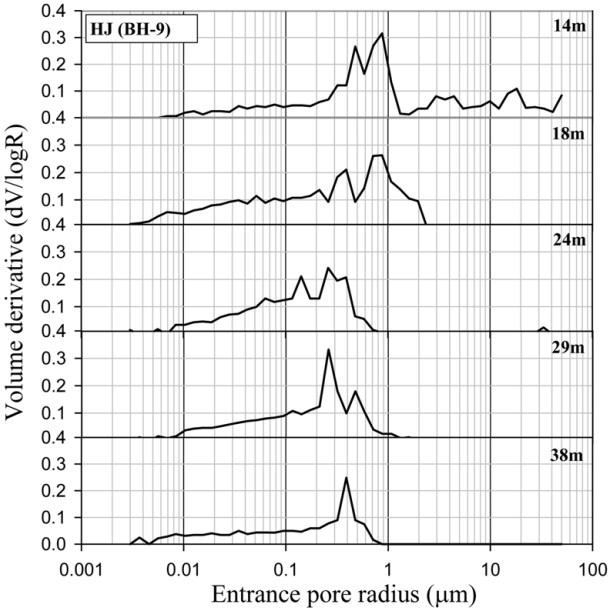

Fig. 6. Pore Size Distributions of Intact Clays at Different Depths

R), where R is the entrance pore size radius and is the volume of pores whose diameter is D_p, expressed in terms of the unit dry weight of soil. Similar to the result of Osaka bay clay (Tanaka et al., 2003), it is observed that as the depth increases, the area under the curve of PSD decreases. It is because the void ratio decreases due to an increase in the effective overburden pressure. One can also see the same trend that the diameter of major pores becomes smaller with increasing depth.

4.2 Pore Size Distribution (PSD) during Consolidation

Fig. 7 presents the pore size distribution curves on samples consolidated under various pressure levels, which were obtained at different depths. It is noted that an increase in the consolidation stress has resulted a decrease in the largest intruded volume. All the curves reveal that the large entrance pore diameter is approximately 1 mm, as shown in the intact clay. As the study of Delage et al (1982), at the first stage that the intrusion pressure were between 40 kPa and 2490 kPa, the mercury filled the largest pores, and then the penetration took place under the pressures between 2,490 kPa and 20,000 kPa. The increase towards very high pressure (20-290 MPa) led to the penetration of pores smaller than 0.05mm in diameter.

The microstructure of clay at the HJ site is shown in Figs. 8(a) and (b), consisting of clay particles and aggregates which are about 2.6 to 10 μm in diameter. Scanning electron microscopy has shown the existence of aggregates including inter-and intra-aggregate pores. It was commonly observed that the inter-

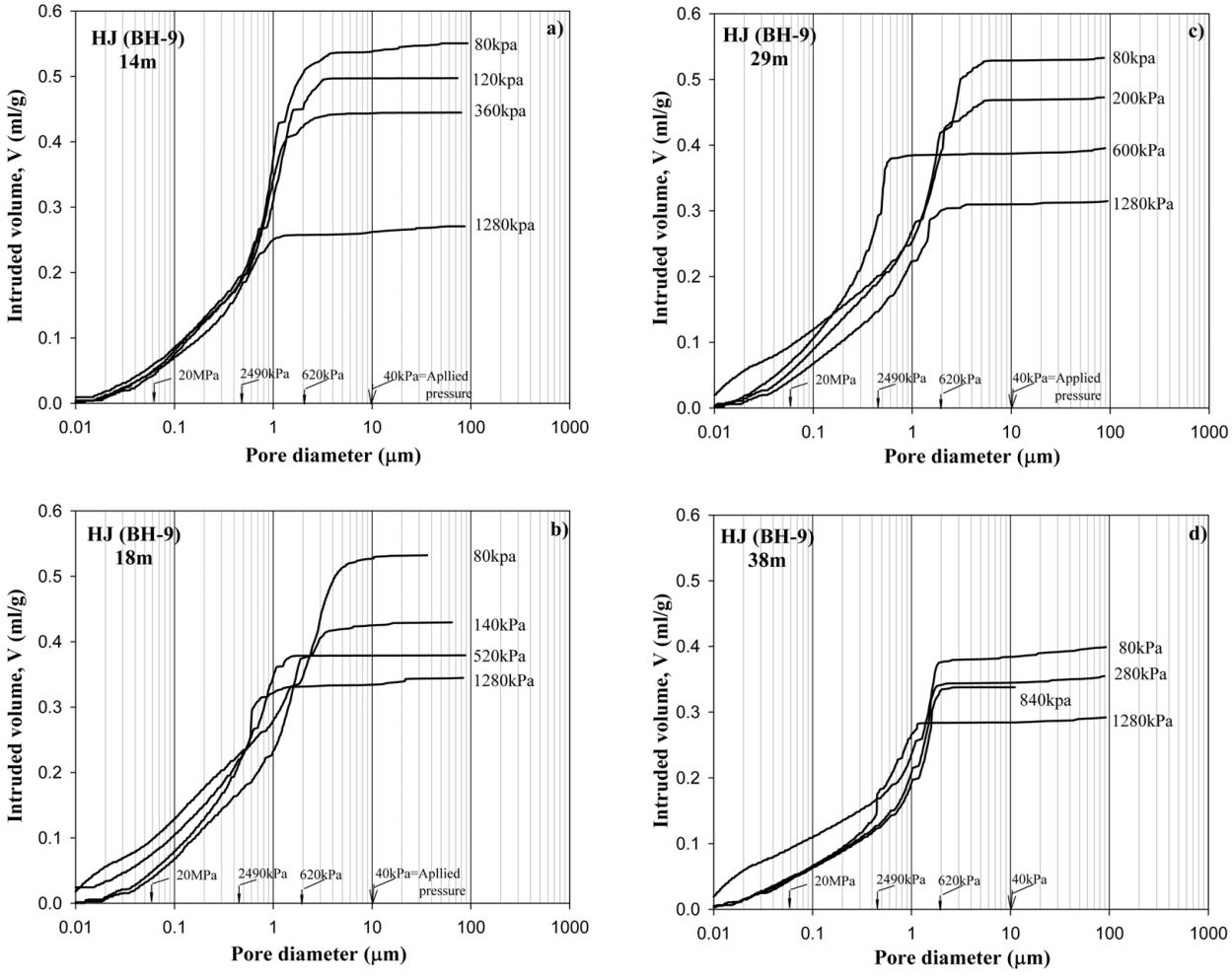

Fig. 7. Mercury Intrusion Curves for Consolidated Samples with Different Pressure Levels, Taken at Various Depths: (a) 14 m, (b) 18 m, (c) 29 m, and (d) 38 m

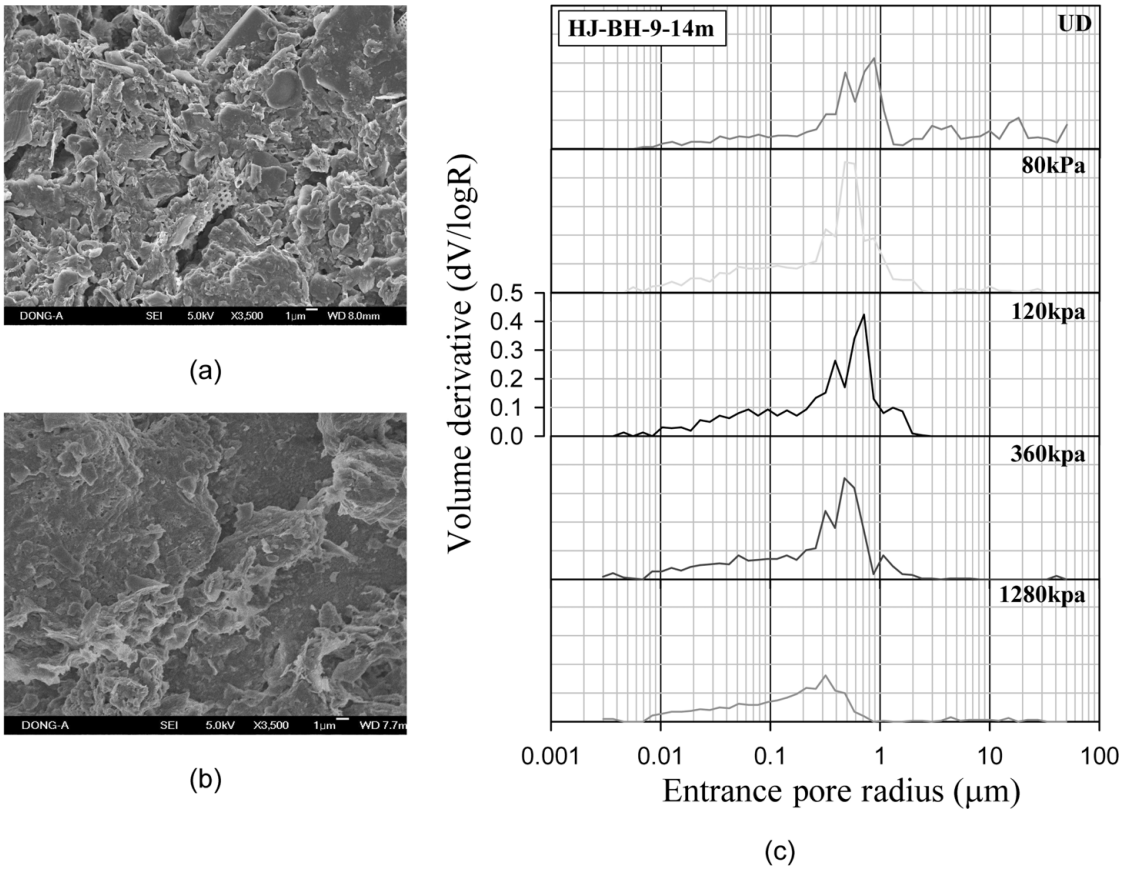

Fig. 8. SEM Pictures of Pusan Clay at the HJ Site: (a) Natural State, (b) Consolidated to 1280kPa, and (c) Various curves showing the evolution of pores during consolidation.

aggregate pore diameter was of the order of 2 μm, corresponding to a pore radius of 1 μm. There is no significant bonding between particles or aggregates. The microstructure for the consolidated sample to 1280kPa indicated that the inter-aggregate pores have essentially decreased in size (Fig. 8b), identical to those shown in Fig. 8(c).

Fig. 9 presents the change in aggregated pore sizes via comparison between the intact and consolidated clays, typically at the depths where represent the upper and lower clays. That is, the change in pore size remarkably took place after the completion of consolidation under a higher stress level (1280 kPa) for the lower clay, as the trend of upper clay shown in Fig. 8(c).

Shown in Fig. 10 is the change in pore diameters due to consolidation on Pusan clay, comparing with those of Japanese clays (Tanaka et al., 2003). It is observed that the values become smaller with increasing the consolidation pressure (σ_{p50}) and an approximately linear relationship between them in logarithm scales exists on Pusan clay. Also, the relationship between σ_v' and D_{p50} varies with samples, indicating that samples having lower compressibility are located above. In the figure, σ_{p50} is diameter at the total cumulative volume of 50%. The Japanese clays have the same trend as Pusan clay, but the lines of Pusan clay are located slightly above those of Japanese clays. The slopes of the lines also vary among the Japanese clays. Therefore, it was recognized that the relationship between σ_v' and σ_{p50} is closely related to the natural characteristics of clays.

4.3 Relation between D_{p50} and Void Ratio

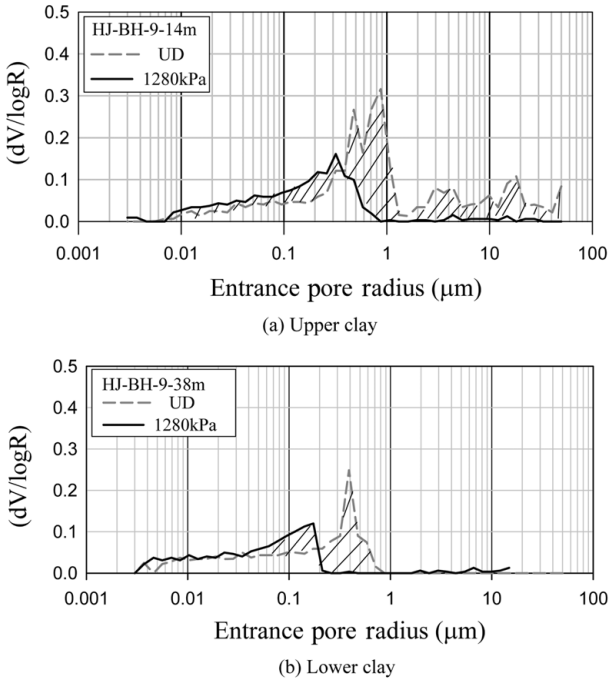

Fig. 9. Pore Size Distribution Curves of Intact and Consolidated Samples at the HJ Site

Fig. 11 shows the relation of void ratio versus D_{p50} for intact Pusan clay (HJ site), comparing with other clays (Tanaka et al., 2003). It is observed that the D_{p50} slightly decreases with the

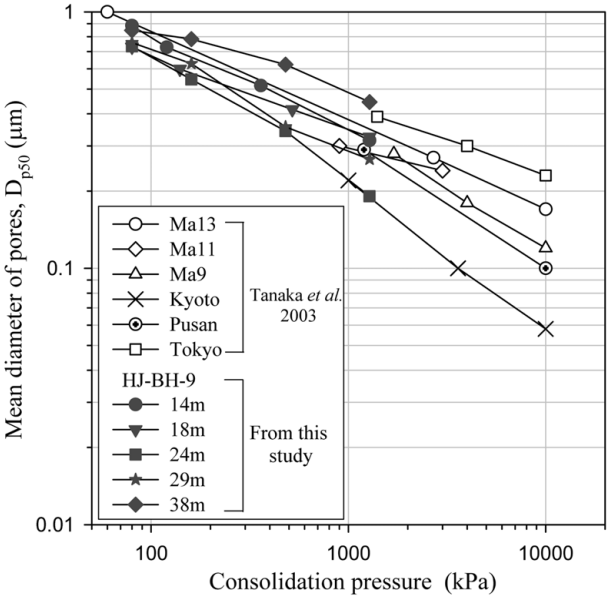

Fig. 10. Comparison of D_{p50} between Pusan and Japanese Clays

decrease in void ratio, showing a large scatter. It was shown that the results from Tanaka et al (2003) and this study for Pusan clay are almost the same as those of Bangkok and Bothkennar clays and are located above that of the Osaka bay clays. This means that the Osaka bay clays tested have relatively smaller pore diameters than the former clays, even at the same void ratio.

Fig. 12 presents the relation between e and D_{p50} in the process of consolidation, comparing with the other clays, where the same data used in Fig. 11 were adopted. As the void ratio decreases due to consolidation, so does the D_{p50}. It can therefore be said that the relation of e vs. D_{p50} for consolidated samples follows the relation measured at the intact condition.

It is well-known that void ratio is one of major factors that affect permeability. Hence, for all the specimens, the void ratios from the oedometer and MIP tests were plotted in Fig. 13. A little discrepancy can be observed, showing that the mercury-intrusion void ratio is largely greater than the IL void ratio. It is probably due to the causes that resulted from the followings:

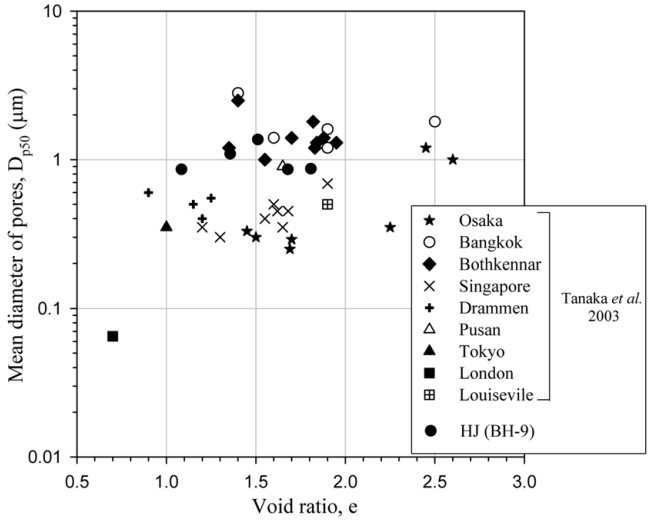

Fig. 11. Relation between e and D_{p50} for In-situ State

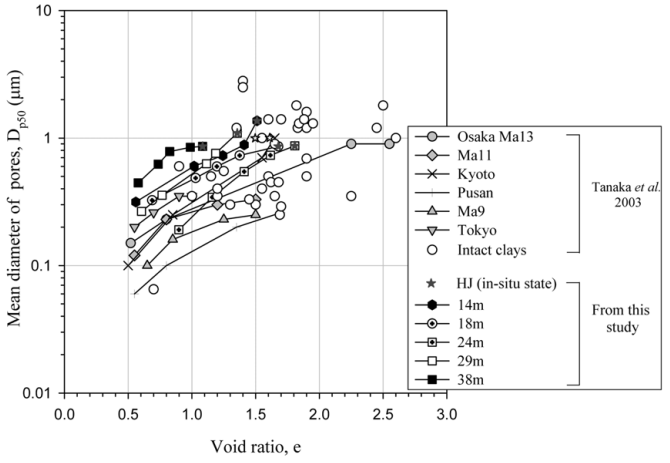

Fig. 12. Relation between e and D_{p50} during Consolidation

expansion of samples retrieved from the oedometer cell after consolidation, measured error of specific gravity, unsaturation of samples for oedometer and MIP tests, etc. Considering that because Pusan clay has low plasticity and OCR of nearly 1.0, samples lead to poor quality, such errors would be unavoidable particularly when oedometer test is performed. Nevertheless, more attention should have been paid for handling samples.

5. Conclusions

The micro-structural investigation on Pusan clay was performed to observe the pore size distribution of the undisturbed and consolidated samples, using the MIP techniques. The results were compared with those of other clays and also correlated with permeability. The following conclusions are drawn through the study.

(1) The cumulative pore volumes reveal difference in the upper and lower Pusan clays. That is, the upper clay has larger

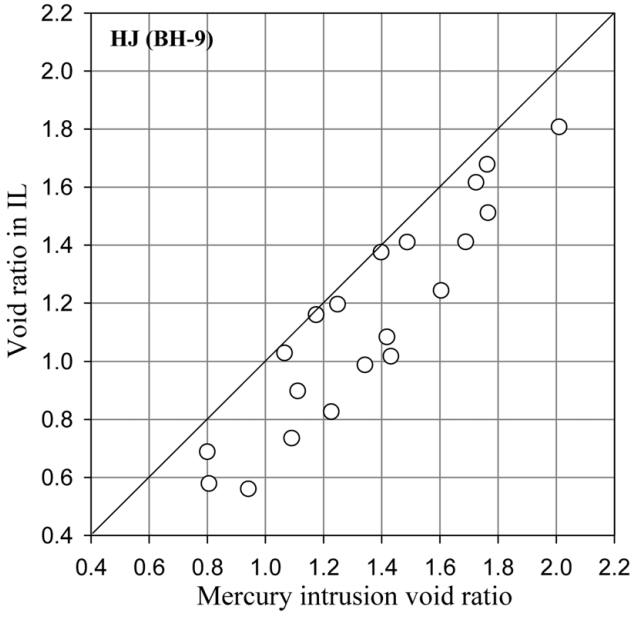

Fig. 13. Comparison of Void Ratios between Oedometer and MIP Tests

pore sizes than the lower clay, because of an increase in the effective overburden pressure σ'_{vo} with depth and different depositional environment. However, it was found that the change in cumulative volume has approximately a similar trend for the upper and lower clays.

(2) Increase in consolidation pressure resulted in a loss of total intruded volume on the clay, because of the deformation of inter-aggregate (large) pore space, as shown in the other clays. That is, only the largest pores (inter-aggregate pores) became smaller, but small intra-aggregate pores were not compressed until the macro pores were collapsed due to the application of large pressures.

(3) The mean diameter of pores, σ_{p50}, was irrelevant to the void ratios for both intact Pusan and other clays, but decreased with decreasing the void ratio during consolidation on all the clays.

Acknowledgement

This study is supported by the Construction Core Technology Program under the KICTTEP and by grant No.R01-2003-000-10375-0 from the Basic Research Program of the South Korea Science and Engineering Foundation.

References

Chung, S.G., Giao, P.H., Kim, G. J., and Leroueil, S. (2002). "Geotechnical characteristics of Pusan clays." *Canadian Geotechnical Journal*, Vol. 39, pp. 1050-1060.

Chung, S.G., Baek, S.H., Ryu, C.K., and Kim, S.W. (2003). "Theme Lecture: Geotechnical characterization of Pusan clays." *Proceeding of Korea-Japan Joint Workshop, Characterization of Thick Clay Deposits, Reclamation and Port Construction*, Busan, Korea, 8-10 April: 3-44.

Chung, S.G., Kwag, J.M., Giao, P.H., Back, S.H., and Prasad, K.N. (2004). "A study of soil disturbance of Pusan clays with reference to drilling, sampling and extruding." *Geotechnique*, Vol. 54, No. 1, pp. 61-65.

Chung, S.G., Ryu, C.K., Jo, K.Y., and Huh, D.Y. (2005). "Geological and geotechnical characteristics of marine clays at the new Busan port." *Marine Georesources and Geotechnology,* Vol. 23, No. 3, pp. 235-251.

Chung, S.G. (2005). "Keynote Lecture: Sampling techniques and their effects in characterizing of Pusan clay." *Proceedings of International Conf on Civil and Environmental Engineering*, ICCEE-2005, Higashi-Hiroshima, Hiroshima University, Japan, Oct 26-27: 29-59.

Chung S.G., Jang, W.Y., Ninjgarav, E., and Ryu, C.K. (2006a). "Compressibility characteristics associated with depositional environment of Pusan clay in the Nakdong River estuary." *Journal of the Korean Geotechnical Society*, Vol. 22, No. 12, pp. 37-65 (in Korean).

Chung S.G., Jang, W.Y., Ninjgarav, E., and Kim, S.R. (2006b). "Permeability characteristics of Pusan clay from laboratory tests." *Journal of the Korean Geotechnical Society*, Vol. 22, No. 11, pp. 133-142 (in Korean).

Delage, P., Tessier, D., and Marcel-Audiguier, M. (1982). "Use of the Cryoscan apparatus for observation of freeze fractured surfaces of a sensitive Quebec clay in scanning electron microscopy." *Canadian Geotechnical Journal*, Vol. 19, pp. 111-114.

Delage, P. and Lefebvre, G. (1984). "Study of the structure of a sensitive Champlain clay and its evolution during consolidation." *Canadian Geotechnical Journa*l, Vol. 21, pp. 21-35.

Garcia-Bengochea, I., Lovell, C.W. and Altschaeffl, A.G. (1979). "Pore distribution and permeability of silty clays." *J. of the Geotech. Engrg., ASCE,* Vol. 105, pp. 839-856.

Juang, C.H. and Holtz, R.D. (1986). "Fabric, pore size distribution, and permeability of sandy soils." *J. of the Geotech. Engrg., ASCE,* Vol. 112, pp. 855-868.

Lapierre, C., Leroueil, S., and Locat, J. (1990). "Mercury intrusion and permeability of Louiseville clay." *Canadian Geotechnical Journal*, Vol. 27, pp. 761-773.

Mesri, G., Kwan Lo, D. O. and Feng, T. W. (1994). "Settlement of embankments on soft clays." *Proc. of Settlement ' 94. ASCE,* Geotechnical Special Publication (40), pp. 8-56.

Ninjgarav, E. (2006). *Consolidation and Permeability Characteristics of Pusan Clay.* PhD Thesis, Dong-A University, Busan, Korea.

Tanaka, H., Dinesh, R., and Tanaka, M. (2003). "Pore Size distribution of clayey soils measured by mercury intrusion Porosimetry and its relation to hydraulic conductivity." *Soils and Foundations* Vol. 43, No. 6, pp. 63-73.

Watabe, Y., Leroueil, S., and Le Bihan, I. P. (2000). "Influence of compaction conditions on pore-size distribution and saturated hydraulic conductivity of a glacial till." *Canadian Geotechnical Journal*., Vol. 27, pp. 761-773.

(Received October 9, 2006/Accepted April 9, 2007)